International Conference on Design and Concurrent Engineering 2012 (iDECON 2012)

October 15–16, 2012
Melaka, Malaysia

Manufacturing Transformation towards Global Sustainability

Organized by

UNIVERSITI TEKNIKAL MALAYSIA MELAKA

Faculty of Manufacturing Engineering
Universiti Teknikal Malaysia Melaka

Supported by

iDECON 2012 – International Conference on Design and Concurrent Engineering
Universiti Teknikal Malaysia Melaka (UTeM)
15-16 October 2012

Regression Model of Processability Properties of Epoxidized Natural Rubber-Alumina Nanoparticle Composites (ENRAN) using Historical Data Design

Noraiham Mohamad[1], Hairul Effendy Ab. Maulod[2], Mohd Shahrizan Othman[1], Mohd Yuhazri Yaakob[1], Andanastuti Muchtar[3], Mariyam Jameelah Ghazali[3], Dahlan Hj. Mohd[4] & Che Husna Azhari[3]

[1] Faculty of Manufacturing, Universiti Teknikal Malaysia Melaka, Hang Tuah Jaya, 76100 Durian Tunggal, Melaka, Malaysia
Phone: +606-3316976, Fax: +606-3316411, Email: noraiham@utem.edu.my
[2] Faculty of Engineering Technology, Universiti Teknikal Malaysia Melaka, Hang Tuah Jaya, 76100 Durian Tunggal, Melaka, Malaysia
[3] Faculty of Engineering & Built Environment, Universiti Kebangsaan Malaysia, 43600 Bangi, Selangor, Malaysia
[4] Malaysian Nuclear Agency, 43000 Bangi, Selangor, Malaysia

Abstract- Response Surface Methodology using Historical Data Design was utilized to develop regression model and analyze the effect of formulation variables on Epoxidized Natural Rubber-Alumina Nanoparticle Composites (ENRAN). ENRANs were prepared through melt compounding with an internal mixer at a temperature of 90 °C and a rotor speed of 60 rpm. Filler loading in the range of 10 phr to 60 phr was chosen as the numerical factor, whereas the presence of silane coupling agent and maleic anhydride was identified as the categorical factor. Processability properties such as cure time, scorch time, maximum and minimum torques, and uniformity were selected as the responses. The significance of the relationship for each regression response was analyzed using ANOVA, and the model's ability to represent the system was confirmed using Fisher test (Test F) and the constant of determination, R^2. ANOVA for each chosen model with confidence levels greater than 99.99% (P-value = 0.0001) showed that the models were accurate in describing and predicting the pattern of significance of each factor studied.

Keywords: Response Surface Methodology, rubber, alumina, processability, historical data design

I. INTRODUCTION

Components based on rubbery materials are crucial and play a very important role in engineering processes and products. In recent years, natural rubber (NR) has been widely used in automobile components, like linings, seals and gaskets [1], engine mounts, gears, cams, and bearings, due to its excellent strength, fatigue resistance, high resilience, and low level of strain sensitivity. It is the elastomer of choice for a majority of applications involving high stress and cyclic flexing. However, NR is characterized by poor resistance to oxygen, ozone, hydrocarbon solvents, and heat. NR is not suitable for many applications that require long-term resistance to continuous temperatures above 100 °C or exposure to oils and solvents [2]. The introduction of epoxidized natural rubber (ENR) in 1922 [3] and the continuous development in the process and properties of elastomeric composites have been the efforts exerted to fill the gaps in the limitations of NR.

ENR is a derivative of natural rubber produced through chemical modification [3] with epoxide groups randomly dispersed along the rubber molecules. Almost like NR, it has the ability to strain crystallize because of the stereospecifity of the epoxidation reaction. Thus, strain crystallizes the epoxide oxygen ENR in its spatial position. Owing to its high miscibility and more polar units [4-5], ENR offers unique properties, such as good oil resistance, low gas permeability, high wet grip, rolling resistance, good damping properties, and significant strength. The oil resistance of ENR 50 vulcanizate has been reported to approach the characteristics of medium-acrylonitrile-content nitrile rubber and to surpass that of CR [4-5]. The resistance to air permeability of ENR 50 has also been claimed to be comparable to butyl rubber and medium-acrylonitrile-content nitrile rubber [4-5]. In addition, inorganic fillers could be more easily dispersed in polar polymers compared with non-polar polymers, such as NR [6-8].

In the manufacture of rubber products, the blending of rubbers and the incorporation of various fillers produce new materials with a wide range of applications because rubbers have potential to combine the attractive properties of their constituent compounds [9]. In addition, numerous choices of inorganic materials are available, whether nano- or micro-sized particles, which can be used to modify the properties of polymeric materials at different volume fractions, shapes, and sizes [10]. Recently, ENR-based elastomeric composites have become an attractive subject of research because of their versatility and ability to be reinforced with various types of fillers and reinforcing phases. Since 1985, extensive studies on incorporating various fillers, such as silica [4,5,11,12], carbon black [13-14], rice husk ash [15-16], chitosan [17], and so on, have been conducted. In recent years, researchers have shifted their focus from micro-sized fillers to nanofillers, owing to the unprecedented combinations of properties observed in some polymer nanocomposites since the "discovery" of carbon nanotubes in the early 1990s [18]. For instance, organoclays [6,8,19], carbon nanotubes [20], alumina

nanoparticles [21-24], and silica nanoparticles [25] have been added to various types of polymers.

Alumina has been recognized as a structural material with an extremely high melting point (2050 □C), high hardness, and capability of forming diverse shapes and functions [26]. The incorporation of nano-scaled alumina has been observed to increase mechanical properties [27] and fracture toughness [28], as well as wear resistance [29], dielectric constant [30], and so on, of the polymer composites. Although conventional alumina is recognized as a commercial material and has been proven to improve the mechanical properties and high thermal performance of polymers, very little literature discusses this issue [30]. Thus, the attempt to produce alumina-composite-reinforced ENR (ENRAN) in our study since [31-33] aims to explore the potential of alumina nanoparticles for use as fillers in the ENR matrix. The effort has also attracted other researchers who compared the performance of micro-sized and nano-sized alumina particles in the NR matrix with the presence of ENR as compatibilizer [23]. The addition of alumina was found to improve the mechanical and oxidation properties of NR, and the properties are further enhanced with the use of alumina nanoparticles. The studies [23,31,33] showed that interactions between the alumina and the rubber matrix exist, as proven by the increase in the crosslink density of the composite.

In the effort to counter NR limitation and offer a material with a new set of properties in manufacturing processes and products, ENR was incorporated with hard, abrasive, and thermal-insulated particles of alumina in our research. This step aims to produce materials with value-added properties, which can be used in applications involving exposure to relatively high temperatures with significant hardness and impact strength, as well as good processability of the materials. Apart from our previous work [31-33], this study tries to establish a mathematical correlation, so called regression model, representing the effects of the formulation (filler loading and chemical modification) to the properties of epoxidized natural rubber-alumina nanoparticle composites (ENRAN). The correlation was done using a statistical tool named "regression analysis" using historical data design through the response surface methodology method. It was done to estimate the quantitative effect of the independent variables upon the response that they influence. Then, the "statistical significance" of the estimated relationships was assessed and justified in terms of the degree of confidence that the true relationship is close to the estimated relationship and the experimental analysis of the samples.

Processability of a composite is highly depending on additional chemicals added into raw materials during processing stage. Various chemicals are incorporated to improve or control either processing or final properties of composites. Silane coupling and compatibility agents are widely used in the rubber industry today. They are believed to promote adhesion through the formation of strong, primary interfacial bonds with both the polymers and the inorganic substrates and to increase the reinforcing ability of inorganic fillers to the rubber matrix [34]. According to Dharmendra et al. [35], the functionalization or surface treatment of the reinforcements with the coupling agents is one of the methods for counteracting the negative effect of fillers on tensile strength. A compatibility agent is a chemical that has two chemical segments: the chemical segment that connects to the polymer, and the chemical segment that connects to other polymers to form covalent bonds between the two phases [36]. The use of compatibility agent will reduce the tendency of phase separation by increasing the adhesion interface of both the matrix and the reinforcements. The coupling and compatibility agents investigated in this study were 3-aminopropyltriethoxysilane [34] and maleic anhydride [37], respectively.

II. EXPERIMENT

A. Materials

Table 1 shows the formulation used in this study. ENR was supplied by Malaysian Rubber Board under the trade name, ENR 50 with a 53% epoxidisation. The average Mooney viscosities measured at ML (1 + 4) 100°C is 85.5 and the average specific gravity at ~25°C is 0.9366. Alumina nanoparticles were supplied by the Nanostructured & Amorphous Materials Inc., USA with an average diameter of 30-80 nm. Other compounding ingredients such as sulphur, zinc oxide, and stearic acid were purchased from Systerm/Classic Chemicals Sdn Bhd.; tetramethylthiuram disulfide (TMTD) from Aldrich Chemistry; N-cyclohexylbenthiazyl sulphenamide (CBS) and N-(1,3-Dimethylbutyl)-N'-phenyl-p-phenylenediamine (6PPD) were supplied by Flexsys America, USA. Both 3-aminopropyltriethoxysilane and maleic anhydride was purchased from Sigma-Aldrich.

B. Preparation & testing of ENRANs

The compounding process was performed according to ASTM D-3192 [31] and carried out using an internal mixer (Haake) working at 90°C and a rotor speed of 60rpm for 6 min [32]. Firstly, ENR was masticated for 1 min before all ingredients except sulphur were added and mixed for another 4 min. Finally, sulphur was added and mixed for about 1 min before the mixture was dumped and cooled down to room temperature.

Determination of cure characteristics on unvulcanized samples

Unvulcanized compounds were rolled into sheets of 0.7 cm thickness using two roll mill at room temperature. Cut samples with weigh approximately 8 g were tested for cure characteristics using a rheometer, Monsanto ODR 2000

from Alpha Technologies based on ASTM D2084-01 (Standard Test Method for Rubber Property-Vulcanization using Oscillating Disc Cure Meter).

Table 1. Typical Formulations.

Ingredients	Loadings (phr)[a]
ENR 50	100
Zinc oxide	2.0
Sulphur	1.6
Stearic acid	1.5
CBS[b]	1.9
TMTD[c]	0.9
6PPD[d]	2.0
SCA[e] (% of alumina)	0.0 or 2.0
MAH[f] (% of ENR)	0.0 or 2.0
Alumina	10, 20, 30, 40, 50, 60

[a] Parts per hundred rubber
[b] N-cyclohexylbenthiazyl sulphonamide
[c] Tetramethylthiuram disulfide
[d] N-(1,3-Dimethylbutyl)-N'-phenyl-p-phenylenediamine
[e] 3-aminopropyltriethoxysilane
[f] Maleic anhydride

Testing and Analysis on vulcanized composites

After 24 h at room temperature [38], unvulcanized compounds were cured into sheets approximately 3 mm thick using a hot press Scientist from LabTech Engineering Company, Ltd., at a temperature of 150 °C and an applied pressure of 100 kgf/cm^2. The curing time was based on the results from the rheometer analysis. The mass of the compound to be molded was estimated from the volume of the mold cavities and the density of the compound. At the end of the molding process, every sample was cooled at 20 °C for 3 min using PAN ASIA Industrial Cooling system, Ltd.

Uniformity of filler distribution was determined from impact fracture surfaces using SEM EVO50 from ZEISS. For each sample, at least three micrographs were taken at magnifications of 500x and 2000x to ensure high confidence level in data analysis. Quadrat method was used to measure the uniformity of filler distribution in the composite through the skewness value [39]. In the quadrat method, the SEM micrograph was divided into 50 grids of square cells. Then, the number of visible particles contained in each cell, Nq, was counted. The skewness or skew value, β, which is the randomness of the particle distribution in the ENR matrix, was calculated according to Eq. 1.

$$\beta = \frac{q}{(q-1)(q-2)} \sum \left(\frac{N_{qi} - N_q^{mean}}{\sigma} \right)^3 \qquad (1)$$

where,
q = the total number of quadrats
N_q = the number of particles contained in i^{th} square; with (i = 1,2, ...q)
N_q^{mean} = the mean of the number of particles per square
σ = standard deviation

A differential scanning calorimetre (DSC) (Perkin Elmer Jade) is used to obtain the T_g of the vulcanized samples with a temperature ramp from -60 to 120 °C at 10 °C min^{-1}. The measurement is performed three times for every sample. The outliers were discarded, and the mean was calculated from remaining values to ensure the validity of the data.

C. Experimental design

Establishment of regression model and analysis were carried out by Response Surface Methodology using Design Expert® software (Stat-Ease Inc., Statistics made easy, Mineapolis, MN, US. Version 6.0.10). Historical data design was selected since the response data was available. Independent variables or factors in this study were loading of alumina particles (X1), chemical modification using SCA (X2), and chemical treatment using MAH (X3) with levels of variables as tabulated in Table 2. The X1 values are numerical factor with value of 10 phr, 20 phr, 30 phr, 40 phr, 50 phr and 60 phr. While X2 and X3 were categorical factors coded with value of 1 and -1 representing the presence or absence of the particular chemical in the formulation. Addition of SCA and MAH to the formulation was 2 percent of the filler loading and 2 per cent of matrix respectively, as shown in Table 1. The responses (dependent variables) involved are the value of maximum torque, MH (Y1), minimum torque, ML (Y2), cure time, t90 (Y3), scorch time, t2 (Y4), and skewness (Y5). Cure charactersitics represented by Y1, Y2, Y3 and Y4 are very important characteristics which define the processability of the compound, the dynamic nature and the degree of filler-matrix interaction in ENRAN. Meanwhile, skewness represents the distribution of alumina particles and indirectly plays a role as an indicator of properties uniformity.

Historical data design in this study consists of 24 sets of experiment with a design matrix listed in Table 3. Each set of experiment represents a different formulation of ENRAN. For example, the experiment number 10 (Table 3) shows the ENRAN formulations at filler loading of 40 phr (coded value = +0.2) with the presence of SCA and absence of MAH.

Table 2. Levels of Variables.

Filler loading	SCA	MAH
(X_1,phr)	(X_2, % filler)	(X_3, % matrix)
10(-1.0)	0(-1)	0(-1)
20(-0.6)	2(+1)	2(+1)
30(-0.2)		
40(+0.2)		
50(+0.6)		
60(+1.0)		

Table 3. Historical Data Design Matrix.

	Coded variable		
Experiment	Filler loading, X_1	SCA, X_2	MAH, X_3
1	-1.0	{ -1 }	{ -1 }
2	-0.6	{ -1 }	{ -1 }
3	-0.2	{ -1 }	{ -1 }
4	0.2	{ -1 }	{ -1 }
5	0.6	{ -1 }	{ -1 }
6	1.0	{ -1 }	{ -1 }
7	-1.0	{ 1 }	{ -1 }
8	-0.6	{ 1 }	{ -1 }
9	-0.2	{ 1 }	{ -1 }
10	0.2	{ 1 }	{ -1 }
11	0.6	{ 1 }	{ -1 }
12	1.0	{ 1 }	{ -1 }
13	-1.0	{ -1 }	{ 1 }
14	-0.6	{ -1 }	{ 1 }
15	-0.2	{ -1 }	{ 1 }
16	0.2	{ -1 }	{ 1 }
17	0.6	{ -1 }	{ 1 }
18	1.0	{ -1 }	{ 1 }
19	-1.0	{ 1 }	{ 1 }
20	-0.6	{ 1 }	{ 1 }
21	-0.2	{ 1 }	{ 1 }
22	0.2	{ 1 }	{ 1 }
23	0.6	{ 1 }	{ 1 }
24	1.0	{ 1 }	{ 1 }

III. RESULTS AND DISCUSSION

From experimental findings, an approximate polynomial relationship for dependent variables (response) was obtained. The result of this design was used to fit a second-order polynomial [40-41] in Eq. (2), which included all interaction terms.

$$Y = \beta_o + \sum_{i=1}^{k}\beta_i x_i + \sum_{i=1}^{k}\beta_{ii} x_{ii}^2 + \sum_{i<j}\sum\beta_{ij} x_i x_j + \varepsilon \quad (2)$$

where Y is the predicted response and ε is a random error. In this study, $k = 3$ was taken since there were three independent variables involved. The mathematical relationship connecting the three variables and the response from Eq. (2) becomes;

$$Y = B_o + B_1X_1 + B_2X_2 + B_3X_3 + B_{11}X_1^2 + B_{22}X_2^2 + B_{33}X_3^2 + B_{12}X_1X_2 + B_{13}X_1X_3 + B_{23}X_2X_3 \quad (3)$$

where, Y is the predicted response; B_0 is the offset term; B_1, B_2, and B_3 are the linear coefficients; B_{11}, B_{22}, and B_{33} are the quadratic coefficients; B_{12}, B_{13}, and B_{23} are the cross-product coefficients; and X_1, X_2, and X_3 are the independent variables. The response surface quadratic model for the studied system consisted of three cubic models (MH, ML and t_2), a quadratic model (t_{90}), and a two-level factorial model (skewness). The model selected for each response was based on the highest priority in accordance with the polynomial level and the lowest P-value. The observed values for each response were compared with the predicted values generated by the software using RSM (Table 4).

Table 4. Experimental and predicted value of response.

No.	Experimental, t_i (dNm)					Predicted, $\hat{t}_i$ (dNm)				
	t_1	t_2	t_3	t_4	t_5	$\hat{t}_1$	$\hat{t}_2$	$\hat{t}_3$	$\hat{t}_4$	$\hat{t}_5$
1	35.45	3.76	2.12	2.12	0.73	34.93	3.69	2.06	1.99	0.65
2	37.64	4.05	2.51	1.56	0.64	36.49	4.29	2.66	1.65	0.63
3	39.91	4.37	2.43	1.49	0.69	39.99	4.61	2.43	1.49	0.68
4	39.6	5.21	2.23	1.3	0.58	39.29	4.84	2.27	1.41	0.65
5	36.61	5.95	2.2	1.27	0.55	36.26	5.65	2.17	1.30	0.59
6	40.39	6.97	2.13	1.17	0.53	40.74	7.13	2.14	1.05	0.55
7	33.69	5.75	1.52	0.54	0.64	33.12	5.00	1.69	0.69	0.47
8	34.97	6.95	1.35	0.37	0.45	36.10	7.24	1.59	0.30	0.49
9	37.47	8.61	1.25	0.21	0.50	37.97	8.83	1.15	0.19	0.53
10	29.65	10.77	1.14	0.23	0.49	29.27	10.14	0.98	0.19	0.52
11	30.05	11.21	1.09	0.23	0.55	31.16	11.56	0.97	0.25	0.54
12	33.77	13.53	0.56	0.16	0.44	34.29	13.46	0.80	0.23	0.35
13	28.59	10.68	4.51	1.31	3.03	29.21	11.17	4.51	1.44	3.04
14	26.58	13.29	4.2	1.23	2.99	25.60	13.14	4.11	1.19	2.97
15	28.97	15.24	3.59	1.23	2.97	28.79	14.54	3.78	1.19	2.93
16	42.85	15.25	3.49	1.23	2.89	42.61	15.75	3.51	1.23	2.83
17	43.53	16.47	3.39	1.52	2.78	44.94	17.14	3.51	1.49	2.77
18	46.29	19.6	3.27	1.49	2.78	47.67	19.09	3.19	1.56	2.73
19	25.41	6.65	4.51	2.24	3.01	25.81	6.45	4.50	2.19	3.08
20	33.63	8.84	4.33	1.5	3.00	33.23	10.47	4.09	1.56	2.97
21	28.79	12.13	3.54	1.14	2.90	28.27	11.63	3.75	1.21	2.94
22	41.79	12.29	3.36	1.23	2.91	41.79	12.21	3.49	1.24	2.90
23	43.49	12.77	3.29	1.23	2.79	44.64	12.90	3.27	1.29	2.87
24	46.3	13.74	3.21	1.26	2.75	47.66	13.76	3.14	1.30	2.80

From the observed values, a regression equation for the selected model for the response, Y, as a function of phr alumina particles (X_1), presence of SCA (X_2), and presence of MAH (X_3) was derived. The regression equation for each response of Y_1, Y_2, Y_3, Y_4, and Y_5 are written in Eqs. (4) to (8). All model terms, whether significant or not, are included in each equation. This mathematical relationship represents the quantitative effects of the independent variables and their interaction effects to the response [42]. In other words, the coefficient is associated with variable effects on the Y value. Coefficients with more than one factor term and coefficients with high factor terms

represent the interaction terms and the quadratic relationships. Positive values reflect an effect that leads to optimization, whereas negative values are factors that give opposite effect on the response [42]. The significance of a constant will be represented by the P-value, also known as a probability > F. Table 5 lists the P-values for each term of the model involved in the regression model selected for each response. A P-value greater than 0.05 reflects a model term that is insignificant.

$$Y_1 = 35.54 + 6.2X_1 - 1.17X_2 - + 5.2X_3 - 1.36X_1^2 - 0.14X_1X_2 + 1.65X_1X_3 + 0.6X_2X_3 + 2.22X_1^3 - 0.27X_1^2X_2 - 1.81X_1^2X_3 + X_1X_2X_3 \quad (4)$$

$$Y_2 = 10.35 + 2.17X_1 + 0.41X_2 + 3.23X_3 - 0.14X_1^2 + 0.29X_1X_2 + 0.15X_1X_3 - 1.97X_2X_3 + 0.98X_1^3 - 0.44X_1^2X_2 - 0.32X_1^2X_3 - 0.94X_1X_2X_3 \quad (5)$$

$$Y_3 = 2.66 - 0.55X_1 - 0.33X_2 + 0.96X_3 + 0.21X_1^2 - 0.008X_1X_2 - 0.13X_1X_3 + 0.31X_2X_3 \quad (6)$$

$$Y_4 = 1.03 + 0.02X_1 - 0.32X_2 + 0.22X_3 + 0.28X_1^2 - 0.07X_1X_2 + 0.08X_1X_3 + 0.32X_2X_3 - 0.28X_1^3 + 0.11X_1^2X_2 + 0.1X_1^2X_3 - 0.19X_1X_2X_3 \quad (7)$$

$$Y_5 = 1.73 - 0.07X_1 - 0.01X_2 + 1.17X_3 + 0.04X_1X_2 - 0.06X_1X_3 + 0.04X_2X_3 \quad (8)$$

Table 5. *P*-value for each model term.

Model Source	Y_1	Y_2	Y_3	Y_4	Y_5
X_1	< 0.0001	0.0004	< 0.0001	0.8811	0.0012
X_2	0.0025	0.0340	< 0.0001	< 0.0001	0.4005
X_3	< 0.0001	< 0.0001	< 0.0001	0.0002	< 0.0001
X_1^2	0.0192	0.6184	0.0228	0.0017	-
X_1X_2	0.6506	0.0963	0.8666	0.1254	0.0238
X_1X_3	0.0001	0.3535	0.0188	0.0645	0.0015
X_2X_3	0.0111	< 0.0001	< 0.0001	< 0.0001	0.0057
X_1^3	0.0379	0.0838	-	0.0526	-
$X_1^2X_2$	0.6052	0.1326	-	0.1505	-
$X_1^2X_3$	0.0035	0.2721	-	0.1779	-
$X_1X_2X_3$	0.0052	< 0.0001	-	0.0006	-

From the regression Eq. (4) and the P-value (Table 5), MH was found to be dependent on the linear terms of X_1, X_2, and X_3, which refer to the total loading of alumina particles, the presence of MAH, and the presence of SCA. Similarly, the squared and cubic terms of X_1 refer to the interaction terms of X_1X_3, X_1X_2, and $X_1X_2X_3$. Nevertheless, the linear terms of X_1 and X_3 showed the highest impact to MH, with positive coefficient values of 6.2 and 5.2, respectively. This result indicates that the addition of alumina particles and MAH, separately or together, will increase the MH value, which is proven by the positive value of the coefficient of interaction term X_1X_3 and the P-value equal to 0.0001. On the other hand, negative value of the X_2 coefficient (- 1.17) shows that the presence of SCA will only reduce the value of MH. Although it was combined with increasing filler loading, the negative effect to MH of the presence of SCA cannot be eliminated. However, the negative effect of SCA can be improved when used in conjunction with MAH or when all three (alumina, SCA, and MAH) are mixed in a formulation of ENRAN. This effect is represented by the coefficients of interaction term X_2X_3 and $X_1X_2X_3$, which were equivalent to + 0.6 and + 1, respectively. However, this effect is more trivial than the individual effect of the alumina particle loading into the ENR matrix because the alumina particles have good compatibility with the ENR matrix, even without chemical treatment. MH represents the effect of the filler reinforcement of a matrix [8]. Hence, increasing the MH value is an indirect indication of the reinforcement effect of alumina particles on the ENR matrix. The reinforcement effect of alumina in ENRAN increased as the filler loading and MAH increased. Nonetheless, this effect was reduced by the addition of SCA into the ENR matrix.

The decreased reinforcement effect in the presence of SCA is contrary to the effect of using silane coupling agents in silica-reinforced rubber composites. One obvious reason is the compounding process. In addition, SCA directly mixed into the mixture is less effective. In most studies, the coupling agents were pre-treated onto filler surfaces before they were added into the mixture during the compounding process [12,43]. The observed decline in MH is also due to the increasing toughening effect when SCA is present in the mixture, as when alumina was added to PMMA [21-22].

For the response Y_2 in Eq. (5), which represents the value of ML, the factor that had the greatest effect was the presence of MAH (X_3), followed by alumina particle loading (X_1), and then by the interaction term between SCA and MAH (X_2X_3). These three terms were + 3.23, + 2.17, and - 1.97, respectively. Most of the interaction and quadratic terms give negative effect to the ML value, except for the interaction of X_1X_2 and X_1X_3. Based on the P-values from Table 5, only four terms (X_3, X_1, X_2, and X_2X_3) are significant factors. The cube graph in Fig. 1 is the effect of the terms X_1, X_2, and X_3 and their interaction with the value of ML. The lowest ML value was obtained at 10 phr alumina particles loading, without SCA and MAH. The results predicted by RSM are in good agreement with the experimental results shown in Fig. 2.

ML represents the melt viscosity. A high ML value indicates high viscosity of the melt material during vulcanization. The presence of MAH is a major factor that plays a role in increasing the ML value of the melt, which is the consequence of the "selective microstructure" that formed in the ENRAN because of the presence of MAH during compounding (Fig. 3). "Selective microstructure" is observed when the material structure is divided into two separate areas of high filler concentration and high matrix concentration. The area of high filler concentration acts as a relatively large body and prevents the movement of macromolecules during the vulcanization process of ENRAN. The obstruction to flow increases the viscosity of rubber melts under an applied force and temperature. Extremely high viscosity of the melt is not practical because of difficulty in the processing and production of materials with non-uniform properties. Although the

presence of SCA also contributes to an increase in viscosity, the effect is lower. This behavior is evident from the uniform distribution of the filler particles on the composite fracture surface (Fig. 3).

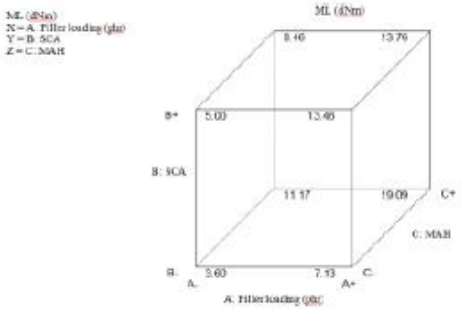

Fig. 1. Cube graph for relationship between parameters and ML value.

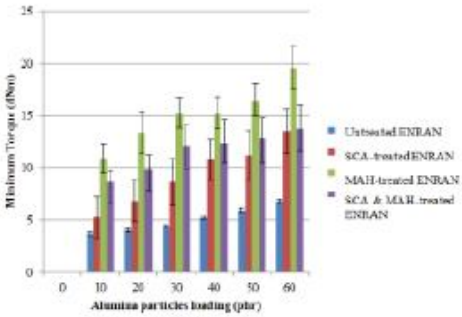

Fig. 2. Minimum torque (ML) at various filler loading of four different ENRAN's system.

For the cure time (t_{90}) or Y_2 response in Eq. (6), the significant terms were X_1, X_2, X_3, X_1^2, X_1X_3, and X_2X_3 (Table 4). This result means that all the three variables are important in the optimization of the t_{90} value. However, the loading of alumina particles and the presence of SCA, either individually or in combination, will only lower the t_{90} value in Eq. (4). This behavior means that both factors act to accelerate the curing reaction of ENRAN during vulcanization. The uniform and small size of the dispersed alumina particles in untreated ENRAN and SCA-treated ENRAN (Fig. 3) play a role in the reduction of the t_{90} value. This result is due to the influence of particle size. The smaller the particle size, the higher the particle surface area available for reaction. Thus, as the rate of the vulcanization reaction becomes faster, the cure time is lessened [15].

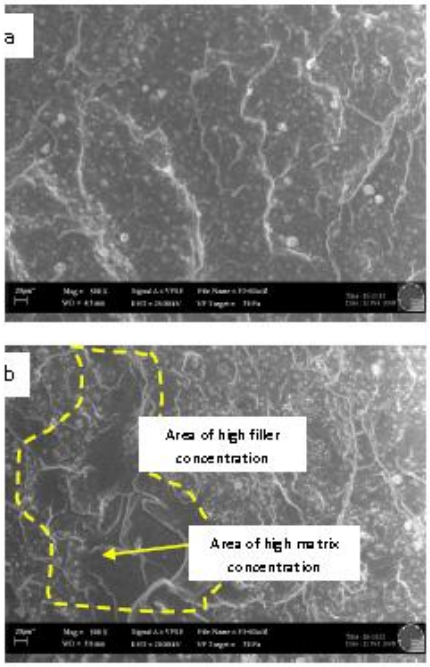

Fig. 3. Comparison of microstructure of (a) ENRAN-60/SCA with (b) ENRAN-60/MAH at magnification of 500x.

The presence of MAH lowered the rate of curing, except when combined with increasing filler loading into the mixture. The t_{90} is inversely proportional to the increase in alumina particles. The presence of MAH is supported by the interaction graph (Fig. 4). Clearly, the value of t_{90} for ENRAN/MAH was 60% higher than untreated ENRAN. However, the negative effect on t_{90} decreases with increasing alumina loading in ENRAN, which is evident from the micrograph comparison in Fig. 6. Increasing the alumina particles reduces the density of the large agglomerates in the material. The addition of SCA with MAH in the mixtures improved the distribution and nature of the dispersed particles (Fig. 6). Thus, the effect of particle size on reaction rate was also reduced. Refering to the cube graph in Fig. 5, the highest t_{90} was obtained in the mixture of alumina particles at minimum loading in the presence of MAH and in the absence of SCA.

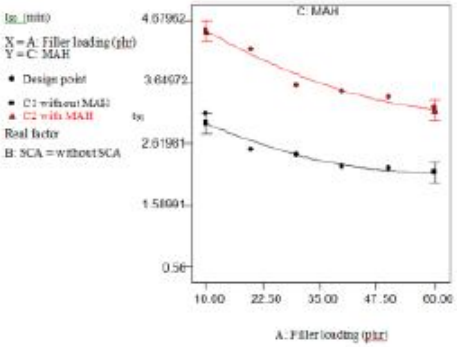

Fig. 4. Interaction graph between factor and t_{90} value.

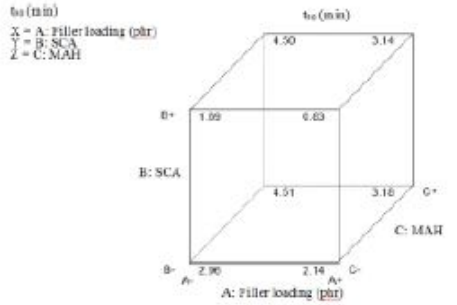

Fig. 5. Cube graph for correlation between parameter with t_{90} value.

Scorch time (t_2) is the time offset during which a rubber compound can be workable at a given temperature before curing begins. An optimal value of t_2 is needed because when t_2 is too low, the rubber compound has inadequate time to fill up the mould, thereby producing products that do not meet the specifications. Based on the generated regression in Eq. (7), t_2 involves the highest polynomial level—a cubic model. Clearly, the relationship among the parameters of the response is complex. As shown in Table 5, X_2, X_3, X_1^2, X_2X_3, and $X_1X_2X_3$ are significant terms with P-values lower than 0.05. Although the linear terms of the alumina particle loading are not significant to the system, the squared term and the interaction terms of X_1, gives the impression that the factor X_1 is still an important factor that increases t_2. As can be seen from the regression model in Eq. (7), increasing the alumina particles lowers the t_2 values in ENRAN, and a similar effect is produced when it is added separately or together with SCA and MAH. However, the presence of MAH can help increase the value of t_2 to 0.22 times, and it shows a positive effect when incorporated with increasing filler loading and when SCA is present. The presence of SCA in the formulation of ENRAN has a negative effect on t_2, unless combined with MAH. This behavior is represented by the interaction graph in Fig. 7. When the loading of alumina particles is fixed at 35 phr, the value of t_2 will be dramatically reduced. If SCA is added to the solution, t_2 increases slightly from the original value, when added together with MAH. This behavior is due to the small particle size and the spherical shape (Fig. 6) that accelerate the reaction in the presence of SCA.

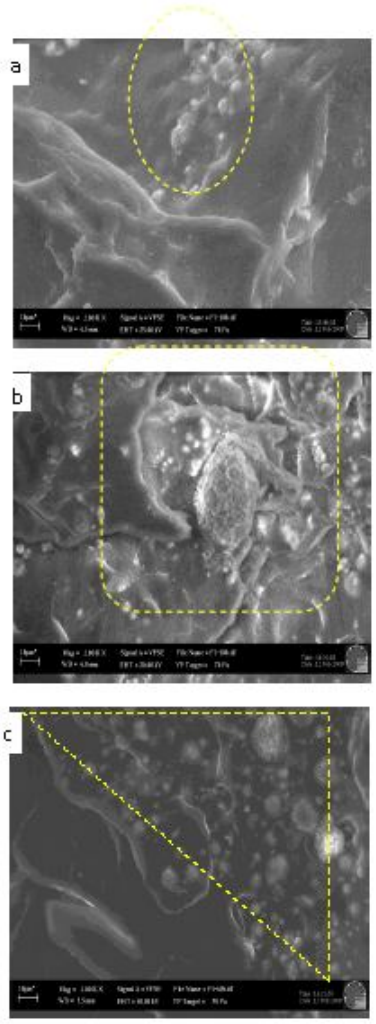

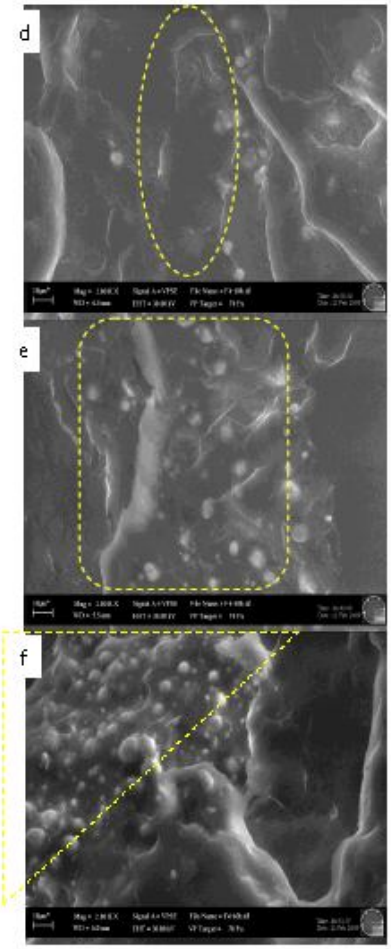

Fig. 6. Changes of distribution, shape and size of dispersed alumina particles in (a) ENRAN-10/MAH, (b) ENRAN-30/MAH, (c) ENRAN-60/MAH, (d) ENRAN-10/SCA/MAH, (e) ENRAN-30/SCA/MAH and (f) ENRAN-60/SCA/MAH. Highlighted areas showed the area of high filler concentration.

Skewness (Y_7) represents the uniformity of the alumina particle distribution in ENRANs and is calculated using quadratic techniques [39]. Skewness (Y_7) is very important in ensuring uniformity of composite properties. Due to the consistency in filler distribution, a two-level factorial model was used to represent the relationship between skewness and the X_1, X2 and X_3 factors. From the mathematical relationship in Eq. (8), only X_1, X_3, X_1X_2, X_1X_3 and X_2X_3 were identified as significant terms by RSM (Table 5). Factor X_3, which represents the presence of MAH, plays an important role in the optimization of the skewness value. The presence of MAH tends to increase the value of Y_7, except when combined with increasing filler loading. This relationship is summarized in the interaction graph (Fig. 8), where Y_7 is reduced by increasing the filler loading. The reduction became more apparent when MAH was added into the compound, whereas the effect of SCA to Y_7 was only in the multiples of 0.04, as in Eq. (8). Although the presence of SCA is able to reduce the dispersed particle size and to produce more spherical particles (Fig. 6), the factor X_2 is mathematically less meaningful to the uniformity of alumina particle distribution in the ENR matrix. RSM predicted that a maximum skewness value as high as 3.04 will be obtained at minimum filler loading in the presence of MAH and without the presence of SCA (Fig. 9). However, high skewness values are undesirable to the system because they reflect high asymmetry and less uniformity of distribution. A value near zero ($\beta \sim 0$) is required in a distribution [39].

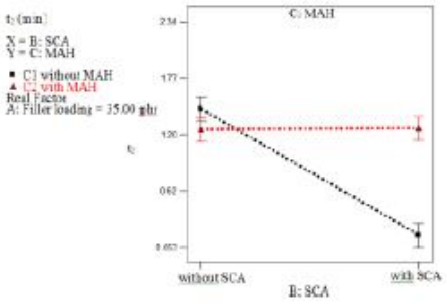

Fig. 7. Interaction graph between the presence of MAH and SCA to the t_3 at constant filler loading.

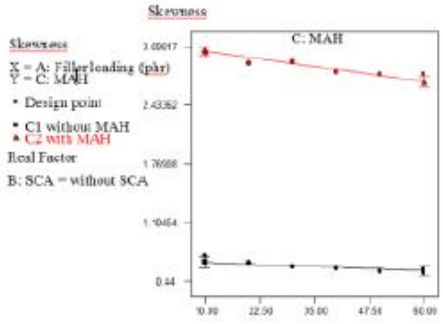

Fig. 8. Interaction graph of filler loading and the presence of MAH to the skewness at constant SCA factor.

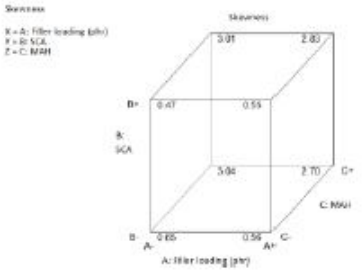

Fig. 9. Cube graph of relationships between factor and skewness value.

Table 6. ANOVA for model of each factors.

	Y1	*Y2*	*Y3*	*Y4*	*Y5*
SS	1287.00	433.75	30.87	7.37	32.91
DOF	11	11	7	11	6
MS	117.00	39.43	4.41	0.67	5.48
F-value	121.74	137.46	170.17	36.56	1699.74
P-value	<0.0001	<0.0001	<0.0001	<0.0001	<0.0001
Standard Deviation	0.9803	0.5356	0.1610	0.1353	0.0568
R^2	0.9911	0.9921	0.9867	0.9710	0.9983
$\|R\|$	0.9830	0.9849	0.9809	0.9445	0.9977

The significance of relationship for each regression response was analyzed using ANOVA, and the model's ability to represent the system was confirmed using the Fisher test (Test F) and the constant of determination, R^2. The details of the ANOVA for each chosen model are listed in Table 6. The analyses show that the confidence level for each model was greater than 99.99% (P-value = 0.0001). The F values for each response were 121.74, 137.46, 170.17, 36.56 and 1699.74, with the probability > F at < 0.0001 [44]. The positive values of F and the low probability > F (P-value) show that each model has good consistency between the observed and the predicted values. Hence, the mathematical relationships of the models are adequate to represent the system under consideration [44], especially as shown by the high coefficients of determination R^2 (i.e., 0.9911, 0.9921, 0.9867, 0.9710 and 0.9983) (Table 6). With the values of R^2 very close to union (R^2 = 1), almost 100% of the variation in the overall system was represented by the model. This result shows that the model is accurate in describing and predicting the pattern of significance of each factor studied. The value of R^2 also exhibited good agreement with the value of the coefficient correlation, |R|.

IV. CONCLUSIONS

The regression model of the processability properties of ENRAN composites was successfully developed through RSM using Historical Data Design. The selected mathematical model was adequate and effective in representing the behavior of the ENRAN composites in terms of processing ability and uniformity in the function of selected independent variables involved in the study. It showed high confidence levels greater than 99.99%, and P-values smaller than 0.05. The predicted responses from the model were in good agreement with the observed and actual analysis data in the laboratory. The selection of a suitable regression model is crucial to ensure the validation of data analysis and the accurate prediction of optimization decision.

ACKNOWLEDGEMENTS

The authors acknowledge the Ministry of Higher Education Malaysia and Universiti Kebangsaan Malaysia (UKM) for granting the Fundamental Research Grant Scheme (UKM-RS-02-FRGS0003-2007) to carry out this project. We wish to sincerely thank the Malaysia Nuclear Agency for providing the equipment and technical assistance to carry out the experiments. The first author is grateful to Universiti Teknikal Malaysia Melaka (UTeM) for granting concession and study.

REFERENCES

[1] Gent, A.N. 2001. Engineering with rubber-How to design rubber components. Ed. ke-2. Munich: Carl Hanser Verlag.

[2] Cancarb. 1999. Properties of thermal black filled EPDM engine mount. Technical Bulletin 019. Canada.

[3] Salamone, J.C. 1996. Polymeric Materials Encyclopedia. Jil. 10. Boca Raton: CRC Press.

[4] Ismail, H. & Chia, H.H. 1998a. The effects of multifunctional additive and epoxidation in silica filled natural rubber compounds. Polymer Testing 17: 199–210.

[5] Ismail, H. & Chia, H.H. 1998b. The effects of multifunctional additive and vulcanization systems on silica filled epoxidized natural rubber compounds. European Polymer Journal 34(12): 1857-1863.

[6] Wu, Y.T., Mark, J.E., Pham, L.Y.H. & Engelhardt, M. 2001. Clay nanolayer reinforcement of cis-1,4-polyisoprene and epoxidized natural rubber. Journal of Applied Polymer Science 82: 1391–403.

[7] Varghese, S., Karger-Kocsis, J. & Gatos, K.G. 2003. Melt compounded epoxidized natural rubber/layered silicate nanocomposites: structure-properties relationships. Polymer 44: 3977-3983.

[8] Teh, P.L., Mohd Ishak, Z.A., Hashim, A.S., Karger-Kocsis J. & Ishiaku, U.S. 2004. Effects of epoxidized natural rubber as a compatibilizer in melt compounded natural rubber–organoclay nanocomposites. European Polymer Journal 40: 2513–2521.

[9] Arayapranee, W.& Rempel, G. L. 2007. Properties of NR/EPDM Blends with or without Methyl Methacrylate-Butadiene-Styrene. International Journal of Materials & Structural Reliability 5(1): 1-12.

[10] Lim, J.C. 2007. Compression and Wear behaviour of composites filled with various nanoparticles. Compos. Part B-E 38: 79-85.

[11] Manna, A.K. De, P.P., Tripathy, D.K., De, S.K. & Dennis, G.P. 1999. Bonding between precipitated silica and epoxidized natural rubber in the presence of silane coupling agent. Journal of Applied Polymer Science 74(2): 389–398.

[12] Manna, A.K., De, P.P. & Tripathy, D.K. 2002. Dynamic Mechanical Properties and Hysteresis Loss of Epoxidized Natural Rubber Chemically Bonded to the Silica Surface. Journal of Applied Polymer Science 84: 2171–2177.

[13] Bandyopadhyay, S., De, P.P., Tripathy, D.K. & De, S.K. 1995. Dynamic mechanical spectroscopic studies on the miscibility of polychloropreneepoxidized natural rubber blend in presence of carbon black filler. Polymer 36 (10): 1979-1984.

[14] Demirhan, E., Kandemirli, F. & Kandemirli, M. 2007. The effects of furnace carbon blacks on the mechanical and the rheological properties of SBR1502 styrene butadiene rubber. Materials and Design 28: 1326–1329.
[15] Ishak, Z. A. M. & Bakar, A. A. 1995. An investigation on the potential of rice husk ash as fillers for epoxidized natural rubber (ENR). European Polymer Journal 31(3): 259-269.
[16] Ishak, Z. A.M. Bakar, A.A., Ishiaku, U.S., Hashim, A.S. & Azahari, B. 1997. An investigation of the potential of rice husk ash as a filler for epoxidized natural rubber: Fatigue behaviour. European Polymer Journal. 33(1): 73-79.
[17] Ismail, H., Shaari, S.M. & Othman, N. 2011. The effect of chitosan loading on the curing characteristics, mechanical and morphological properties of chitosan-filled natural rubber (NR), epoxidised natural rubber (ENR) and styrene-butadiene rubber (SBR) compounds. Polymer Testing 30(7): 784–790.
[18] Ajayan, P.M., Schadler, L.S. & Braun, P.V. 2003. Nanocomposite Science and Technology. Weinheim: WILEY-VCH Verlag GmbH & Co. KGaA.
[19] Chen, B. & Evans J.R.G. 2008. Impact and tensile energies of fracture in polymer–clay nanocomposites. Polymer 49: 5113–5118.
[20] Sharmugharaj, A.M.; Bae, J.H.; Lee, K.Y.; Noh, W.H.; Lee, S.H.; Ryu, S.H. Physical and chemical characteristics of multiwalled carbon nanotubes functionalized with aminosilane and its influence on the properties of natural rubber composites; Compo Sci & Tech; 2007, 67, 1813–1822.
[21] Siegel, R.W., Chang, S.K., Ash, B.J., Stone, J., Ajayan, P.M., Doremus, R.W. & Schadler L.S. 2001. Mechanical behavior of polymer and ceramic matrix nanocomposites. Scripta materials. 44: 2061–2064.
[22] Ash, B.J., Schadler, L.S. & Siegel, R.W. 2002. Glass transition behaviour of alumina polymethylmethacrylate nanocomposites. Materials Letters 55: 83-87.
[23] Konar, B.B., Roy, S.K. & Pariya, T.K. 2010. Study on the effect of nano and active particles of alumina on natural rubber -alumina composites in the presence of epoxidized natural rubber as compatibilizer. Journal of Macromolecular Science, Part A 47(5): 416 -422.
[24] Fu, J.F., Chen, L.Y., Yang, H., Zhong, Q.D., Shi, L.Y., Deng, W., Dong, X., Chen, Y. & Zhao, G.Z. 2012. Mechanical properties, chemical and aging resistance of natural rubber filled with nano-Al2O3. Polymer Composites 33(3): 404–411.
[25] Park, S.J., Jin, S.Y., Kwang, S. Influence of thermal treatment of nano-scaled silica on interfacial adhesion properties of the silica/rubber compounding; Mater Sci & Eng A: 2005, 398, 137–141.
[26] Ichinose, N. 1987. Introduction to Fine Ceramics (Application in Engineering). Chichester, United Kingdom: John Wiley & Sons Ltd.
[27] Jung, C.H.; Choi, J.H.; Lim, Y.M.; Jeun, J.P.; Kang, P.H.; Nho, Y.C. Preparation and Characterization of Polypropylene Nanocomposites Containing Polystyrene-grafted Alumina Nanoparticles; J. Ind. Eng. Chem.: 2006, 12, 6, 900-904.
[28] McGrath, L.M., Parnas, R.S., King, S.H., Schroeder, J.L., Fischer, D.A. & Lenhart, J.L. 2008. Investigation of the thermal, mechanical, and fracture properties of alumina epoxy composites. Polymer 49: 999-1014.
[29] Bhimaraj, P., Burris, D.L., Action, J., Sawyer, W.G., Toney, C.G., Siegel, R.W. & Schadler, L.S. 2005. Effect of matrix morphology on the wear and friction behavior of alumina nanoparticle/poly(ethylene) terephthalate composites. Wear 258: 1437–1443.
[30] Zhang, C., Mason, R. & Stevens, G.C. 2005. Dielectric Properties of Alumina-Polymer Nanocomposites. Annual Report Conference on Electrical Insulation and Dielectric Phenomena: 721-724.
[31] Mohamad N, Muchtar A, Ghazali MJ, Dahlan HM, Azhari CH. 2008. The effect of filler on epoxidized natural rubber-alumina nanoparticles composites. Euro J of Sci Res. 24(4): 538-47.
[32] Mohamad N, Muchtar A, Ghazali MJ, Dahlan HM, Azhari CH. 2009. Epoxidized natural rubber-alumina nanoparticle composites: optimisation of mixer parameters via response surface methodology (RSM). J of App Poly Sci. 115(1): 183-9.
[33] Mohamad N, Muchtar A, Ghazali MJ, Dahlan HM, Azhari CH. 2010. Correlation of filler loading and silane coupling agent on the physical characteristics of epoxidized natural rubber-alumina nanoparticles composites. J of Elas & Plas. 42: 331-346.
[34] Jia QX., Wu YP., Wang YQ, Lu M, Zhang LQ. Enhanced interfacial interaction of rubber/clay nanocomposites by a novel two-step method. Compo Sci and Tech. 2008; 68: 1050–6.
[35] Dhamendra KS., Subramanyam VK, Venkitanarayanan P. Epoxy composites using functionalized alumina platelets as reinforcements. Compo Sci and Tech. 2008; 68: 3055–63.
[36] Ismail, H.. 2004. Komposit Polimer; diperkuat pengisi dan gentian pendek semula jadi. Minden: Penerbit Universiti Sains Malaysia: 1-127.
[37] Halim, S. F., Ahmed I. Abou-Kandil A. Awad & Darwish N. 2009. In situ Grafting of Maleic Anhydride onto Natural Rubber to Improve Its Adhesion to Polyester Fabric: Mechanical and Spectroscopic Analyses. Journal of Adhesion Science and Technology 23: 71–83.
[38] Morton, M. 1987. Rubber Technology. Edisi Ke-3. New York: Van Nostrand Reinhold Company.
[39] Kamexis, P.A., Durrant, G. & Cantor, B. 1998. Characterization of reinforcement distribution in cast Al-Alloy/SiC composites. Materials Characterization. 40: 97–109.
[40] Myers, R.H. & Montgomery, D.C. 2002. Response Surface Methodology, process and product optimization using designed experiments. Ed. ke-2. Canada: John Wiley & Sons, Inc.
[41] Rosnanida, R.A., Rosli, M.I., Mohd Ghazali, M.N., Fauzi, A.I., Osman, H. & Kamaruzaman, K. 2004. Optimisation of growth medium for the production of cyclodextrin glucanotransferase from Bacillus stearothermophilus HR1 using response surface methodology. Process Biochemistry 39: 2053–2060.
[42] Palamakula, A., Mohammad, T.H.N., & Marsoor, A.K. 2004. Response Surface Methodology for Optimization and Characterization of Limonene-based Coenzyme Q10 Self-Nanoemulsified Capsule Dosage Form. AAPS PharmSciTech 5 (4): 66.
[43] Ismail, H., Rozman, H.D., Jaffri, R.M. & Ishak, Z.A.M. 1997. Oil palm wood flour reinforced epoxidized natural rubber composites: the effect of filler content and size. European Polymer Journal. 33(10-12): 1627-1632.
[44] Salwanis, W.W.M.Z., Rosli, M.I. Madihah, M.S., Osman, H, Rosnanida, A.R., & Aidil, A.H. 2007 Production of cyclodextrin glucanotransferase from alkalophilic Bacillus sp.TS1-1: Optimization of carbon and nitrogen concentration in the feed medium using central composite design. Biochemical Engineering Journal 33: 26–33.